Study of shear and elongational flow of solidifying polypropylene melt for low deformation rates

V. Kitoko, M. Keentok and R. I. Tanner*

School of Aerospace, Mechanical and Mechatronic Engineering, University of Sydney, NSW 2006, Australia

(Received, November 12, 2002; final revision received April 28, 2003)

Abstract

An experimental technique was developed to determine the strain-rate in a tensile specimen. Then one can calculate the transient isothermal elongational viscosity. Both shear and elongational viscosities were measured to study the effect of shear and elongational fields on the flow properties. The comparison between these viscosities shows that the onset of rapid viscosity growth as crystallization solidification proceeds occurs at about the same value of time at very small deformation rates (0.0028 and 0.0047 s^{-1}). The comparison of these measured viscosities as functions of shear and elongational Hencky strains also reveals that the onset of rapid viscosity growths starts at critical Hencky strain values. The behaviour of steady shear viscosity as function of temperature sweep was also explored at three different low shear rates. Finally, the influence of changing oscillatory frequencies and strain rates was also investigated.

Keywords : shear and elongational viscosities, low deformation rates, critical Hencky-strain values, crystallization

1. Introduction

The importance of the injection moulding technology as one of the major mass production methods of plastic articles is well known. During the last two decades, numerous studies, for example (Kumaraswamy *et al.*, 1999), have pointed out that the quality of the mouldings obtained through this technology is strongly dependent on the processing conditions (including the machine set-up and geometrical aspects of the dies). These studies have also shown that, in injection moulding operations, the molten polymer is subjected to intense shear plus an elongational flow field and often crystallizes during or subsequent to the imposition of flow; flow appears to increase crystallization.

With regard to shear induced crystallisation from the melt, a number of other experimental studies (e.g. Han, 1974) have indicated that due to the high shear rates occurring in the injection moulding process [typically, $10^2 - 10^4$ s^{-1}] strongly oriented layers are induced.

However, in particular, it was also shown in the mid-1960s that the application of a small shear strain to a supercooled melt significantly increased the rate of subsequent quiescent crystallisation for polypropylene (Lagasse and Maxwell, 1976).

Based on this idea, Wolkowicz (see Vleeshouwers and Meijer, 1996) showed that lower shear rates also enhance crystallisation, but do not influence the crystal growth speed, and a spherulitic morphology is induced. Vleeshouwers and Meijer (1996) used an oscillatory mode rheometer to examine the influence of low shear rates on crystallisation. They showed that the enhancement of crystallization by low shear rates (<12 s^{-1}) is partly caused by orientation of molecules in the melt. Similar work was recently reported by Wassner and Maier (2000), who investigated the influence of small shearing rates on the isothermal crystallisation behaviour of three different isotatic polypropylenes (i-PP) using a conventional stress-controlled rotational rheometer and an optical shear cell in combination with a light microscope. They concluded that even at relatively low shear rates shear-induced crystallization can be observed. Contrary to Wolkowicz, they clearly showed that under shearing no large spherulites grew, but only very small structures or nuclei were induced and the number of these structures grew tremendously during the crystallization process. The influence of shearing on crystallization has also been considered by Chai *et al.* (2003) and Koscher and Fulchiron (2002).

Flow in converging or diverging regions of dies and moulds as well as flow at the moving front during mould filling can have extensional components. These deformations play a significant role in melt rheology because of their capability to orient polymer molecules and asymmetric particles, which can have a strong effect on final product properties. Few constant strain-rate extensional measurements have been made in the past, and although

*Corresponding author: rit@aeromech.usyd.edu.au

the importance of extensional measurements is now well recognized, there are relatively few data available; it is difficult to generate homogeneous extensional flow. Many different experiment methods have been tried to generate simple uniaxial extension. In most previous work the sample geometries were adapted from the conventional methods used for solids, particularly those for rubber, which simply pull on a rod of fluid.

In this work, the influence of low elongational strain rates on the extensional viscosity of molten polypropylene was investigated on an Instron rheometer. The influence of low shear rates was also explored using a shear controlled-strain rheometer (Bohlin-Vor). Both experiments were compared to investigate the effect of small elongational and shear fields on the flow properties (viscosities). The influence of a temperature sweep on the steady viscosity at different low shear rates was also considered. In addition, the effect of oscillatory shear rates and frequencies on dynamic viscosity is included. A review of oscillatory measurement is given by Tanner (2002b). The increase of elongational and steady (or dynamic) shear viscosities was taken as the indicator for the onset of crystallization (Boutahar et al., 1998).

2. Rheological behaviour of polymers

Polymer melts exhibit complex rheological behaviour, which is shown by their non-linear mechanical properties. We consider the deformation rates used in this work to be small (slow) and also assume the flow to be isothermal and incompressible. We shall consider the shear viscosity, η_s, the moduli G' and G'', the loss tangent, $\tan\delta = G''/G'$, and the elongational viscosity, η_E. The shear rate is denoted by $\dot{\gamma}$, the frequency of oscillation is ω and the elongational rate is $\dot{\varepsilon}$ (see Tanner, 2000).

We note that for a fluid at very slow deformation rates the steady elongational viscosity value should be exactly three times the steady shearing viscosity and this can be expressed mathematically as follows:

$$\lim_{\dot{\varepsilon}\to 0}\eta_E(\dot{\varepsilon}) = 3\lim_{\dot{\gamma}\to 0}\eta_S(\dot{\gamma}) \tag{1}$$

2.1. Crystallization mechanisms and nucleation theory

Crystallization is a phenomenon occurring during the injection moulding process of polymer melts. In reality, this phenomenon takes place when the system is cooled below the equilibrium melting point, T_m. The difference between the melting temperature at the rest condition and the crystallisation temperature is a measure of supercooling, which in turn depends on the cooling rate. The crystallisation can also be considered in a global manner, in an approach integrating nucleation and growth mechanisms as well as growth geometry (Tanner, 2002a). Accordingly, it

is therefore necessary to give the principal elements of the relevant theories used to describe the two different stages of polymer crystallization; these are nucleation and growth.

The classical nucleation theory (Lauritzen and Hoffman, 1960) provides a general formalism to treat the problems of crystalline nucleation. The basic assumption is that at any temperature, at which the liquid phase exists, either in a stable $(T \geq T_m)$ or in a metastable (undercooling, $T < T_m$) state, thermal fluctuations within the liquid may create zones from which crystals can appear. These zones are called nuclei. When a nucleus is formed there is an initial increase in the free energy due to the need to create new surface. As the nucleus grows larger the free energy eventually reaches a maximum value and then decreases until it becomes negative leaving a stable nucleus. Nucleation theories thus depend on being able to determine the free energy of a growing nucleus along any particular path. The simplest case is homogeneous nucleation where nuclei appear spontaneously, due to thermal fluctuations in the liquid phase, without the help of any substrate or external nucleating particles; in practice it is most unusual to find such behaviour. In most cases heterogeneous nucleation is observed, in which nuclei are formed on the surface of foreign bodies or crystals of the same material (self-seeding) already present in the undercooled liquid. This foreign surface will affect the free energy balance, usually so as to increase the rate of nucleation, thus preventing the observation of true homogeneous nucleation.

A major result of classical nucleation theory is the concept of critical nucleus. At any temperature below the equilibrium melting temperature, there exists a critical nucleus size, which is the boundary between two types of behaviour. If the nucleus has a size smaller than the critical one (subcritical nucleus), it is unstable, meaning its probability of decrease is higher than its probability of growth. On the contrary, if the critical size is overstepped, the growth probability of the nucleus is greater than its probability of decrease: such a nucleus is called supercritical or active. The nucleation process is of the greatest importance in determining crystalline morphology. The number and distribution of the nuclei can profoundly affect the orientation and properties of the material after solidification. A trivial example is that if the number of nuclei is very low then in a real production process, the cycle time becomes rather long, the crystallite size becomes very large and the materials are usually brittle. Indeed, in most of the examples there has been a deliberate attempt to control the properties of polymeric materials through control of the nucleation process. An understanding of the theories of nucleation and growth that occur in polymer processing is necessary for the proper appreciation of the relationships between structure and properties.

The kinetic theory of growth, developed by Hoffman and Lauritzen (1961), is based on the concept of nucleation-

controlled growth, which represents the development of nuclei into observable crystals and is able to interpret a number of experimental facts: first, growth involves only the lateral faces of the nucleus. Secondly, the necessity of a sufficient undercooling for growth, which is associated with secondary nucleation and finally the existence of different growth regimes is often related to morphological changes (tertiary nucleation). In flow, the nuclei grow dependent on the thermo-mechanical history which they experience; if the nuclei are sufficiently strained they will grow into threads, otherwise they stay spherical and will further grow radially. In these, so called spherulites, the lamellae are present like twisted spokes in a sphere, while thread-like nuclei grow mainly perpendicular to the thread (Keller and Kolnaar, 1997). Thus, the influence of flow in enhancing crystallization follows.

2.2. Flow induced crystallization

Classical nucleation theory can also be applied to polymer melts during the moulding process, but the strong anisotropy of polymer crystals, directly related to the anisotropy of the macromolecular structure, has to be taken into account. For this reason, the crystallisation behaviour of polymers during the moulding process provides an efficient way of packing molecules. The efficient packing raises the density and also increases interchain attraction so that mechanical properties may be enhanced (Cunha et al., 2000).

Crystallisation under quiescent conditions is a phase transformation process, which is caused by a change in the thermodynamic state of the system. This change can be a lowering of the temperature or a change in the hydrostatic pressure.

In flow, chain extension can occur, as explained in the previous section. Thermodynamically, chain extension will increase the opportunity of crystal formation by increasing the melting point, while kinetically the extended chain is closer to a crystal state than a random chain. By stretching the polymer chains, the rate of crystallization increases. It has been shown by Bashir et al. (1984) and Mackley et al. (1975) that the high-end tail of the molecular weight distribution promotes the formation of extended chain crystals. Following Bashir et al., these high-end tail molecules are stretched out while the rest remains practically unchanged; a stronger elongational rate results in a broader part of the molecular weight distribution being extended. The elongational rate, therefore, determines the amount of oriented molecules (extended chain crystals) present. It has also been suggested by Petermann et al. (1979) that a certain strain and strain rate have to be present for shear flow to induce noticeable crystallization. This means after a nucleus has been formed, continuous crystallization of polymers is kinetically controlled; the motion involved refers to the transport of molecules from the disordered liq-

uid phase to the ordered solid phase, and to the rotation and rearrangement of the molecules at the surface of the crystal, similar to quiescent crystallization. Thus, the influence of these parameters on crystallization needs to be mentioned.

2.3. Influence of strain and strain-rate

Deformation (strain) and deformation rate are two of the most important parameters in the flow-induced crystallisation of polymer melts. As mentioned in the preceding section, the extent of orientation of the polymer molecules, and stability of the resulting orientation-induced nuclei, depend on both the level of the deformation (strain) and the deformation rate (shear rate or elongation rate) relative to the relaxation behaviour of the polymer chains in the melt, which is a major factor governing the overall dynamics of polymer molecules in the melt. These parameters must be high enough to orient and align the polymer chains in the melt to form stable nuclei in the flow direction. At low strains, even at high shear rates, the orientation and alignment of polymer chains are not sufficient to form nuclei. At low shear rates, even at high strains, the oriented chains have sufficient time to relax, and stable nuclei cannot be formed. Thus, at a given strain, the oriented fraction in the polymer crystallised after deformation is expected to be higher at high shear rates than at lower ones.

We can express deformation in terms of length change. This is described by the Cauchy-Green tensor as follows (Tanner, 2000):

$$C = F^T \cdot F \tag{2}$$

where F is called the deformation gradient tensor and F^T its transpose.

Consider first uniaxial elongational flow. Integration of this from the initial coordinate at $t = 0$, X_i, to the coordinate at time t, x_i, results in

$$x = Xe^{\dot{\varepsilon}t}; \quad y = Ye^{-\frac{\dot{\varepsilon}}{2}t}; \quad z = Ze^{-\frac{\dot{\varepsilon}}{2}t} \tag{3}$$

Since $F^T = \frac{\partial x}{\partial X}$ (Tanner, 2000), we have

$$C = \begin{bmatrix} e^{2\dot{\varepsilon}t} & 0 & 0 \\ 0 & e^{-\dot{\varepsilon}t} & 0 \\ 0 & 0 & e^{-\dot{\varepsilon}t} \end{bmatrix} \tag{4}$$

We can then express the strain (Hencky strain) as

$$\varepsilon = \frac{1}{2}\ln C_{max} = \dot{\varepsilon}t \tag{5}$$

where is the magnitude of the largest component of C. In case of simple shear deformation we get

$$x = X + \dot{\gamma}tY, \quad y = Y, \quad z = Z \tag{6}$$

Thus, the shear strain tensor C is derived as

$$C = \begin{bmatrix} 1 & \dot{\gamma}t & 0 \\ \dot{\gamma}t & 1+\dot{\gamma}^2t^2 & 0 \\ 0 & 0 & 1 \end{bmatrix} \quad (7)$$

Accordingly, one can use the Mohr circle to find the largest principal strain and hence the Hencky strain is expressed by

$$\varepsilon = \frac{1}{2}\ln C_{max} = \frac{1}{2}\ln\left(1+\frac{\dot{\gamma}^2t^2}{2}+\dot{\gamma}t\sqrt{1+\frac{1}{4}\dot{\gamma}^2t^2}\right) \quad (8)$$

When the strain is small, in the sense that the fluid particles remain close to their original positions in the reference configuration at all times, then terms of order $\varepsilon^2_{max} = O(\dot{\gamma}^2t^2)$ or higher can be neglected. Then,

$$\varepsilon = \frac{1}{2}\ln C_{max} \approx \frac{1}{2}\dot{\gamma}t \quad (9)$$

For large $\dot{\gamma}t$, we find

$$\varepsilon = \ln(\dot{\gamma}t) \quad (10)$$

3. Experimental methods

Two different types of apparatus were used for determining the rheological properties. A conventional strain-controlled rotational rheometer (Bohlin-VOR) was used in the cone-plate configuration for the steady and dynamic viscosities to be measured under simple steady shear and oscillatory shear deformations and an extensional rheometer (Instron) was also used in the parallel plate configuration to measure the load growth under elongational deformation. Experimental set-ups, including material used, types of flow, procedures and methods used to measure the true elongational rate and to calculate the true elongational viscosity, are described in this section.

3.1. Material

The material used for this study was a polypropylene supplied by Montell-Australia in the form of pellets under the reference ZMA6170P. This is an ultra high flow impact copolymer with a modified molecular weight distribution and is formulated with a general purpose additive package. Such a copolymer is a grade designed for injection molding applications requiring very easy mould filling, low warpage, and good impact/rigidity balance. End use products typically made from ZMA6170P include thin walled containers and refrigerator packaging ware. It was chosen here because the present work was included in a project concerning injection moulding in collaboration with the Materials group at Monash University and also the software company (Moldflow). Both groups are using the same material for their research.
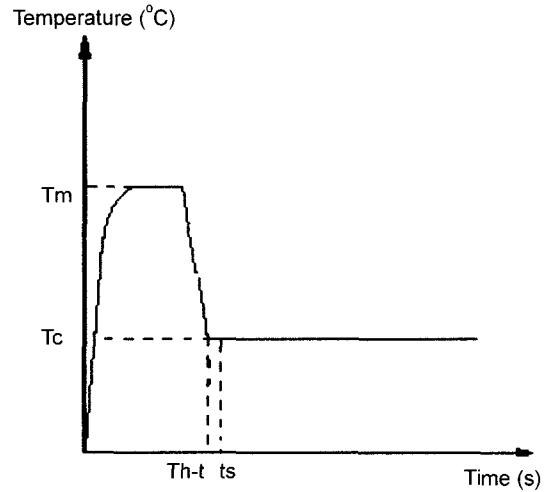

Fig. 1. Temperature-Time sequence of the isothermal crystallization experiment.

3.2. Experimental procedures

Shear (steady and oscillatory) and extensional tests were carried out at different very low constant deformation rates, frequency or strain-rates ranging between 0.003 – 0.01 1/s. The sequence of events in these experiments is summarized in Fig. 1. First, the sample temperature measured by a thermocouple was rapidly raised to a peak melting temperature (T_m) of about 20°C above the equilibrium melting point of this polymer (230°C) to ensure that any memory of the melt is erased. After five hundred seconds of holding the temperature at 250°C (annealing period), the sample was slowly quenched at the rate of 48°C/min to the desired crystallization temperature $(T_c=130°C)$. Following 120 seconds of equilibration period (Th-t), shearing was initiated (t_S), and thereafter the sample temperature remained constant to within ±1°C.

When shearing was initiated, the usual transient or overshoot effects were evident in the measured melt viscosity. After a time, the material recovered and the viscosity stabilized to a constant value until crystallization began. The onset of crystallization during shear flow was detected by a rise in melt viscosity, which took place during isothermal shear flow. The same procedure was used for the elongational experiment, the only difference being that the extensional rheometer was used to measure the load growth during uniaxial elongation at constant extensional-rate. A digital camera monitored the deformation of the sample through all the experiments. Special attention was paid to the illumination to avoid shadows and give a good contrast at the specimen borders. The camera images were transferred into a computer and then used to measure the true diameters through image analyzer software. The variations of the diameter at different times were fitted by a double decay exponential equation. This is therefore used to extrapolate the average true strain-rate value of the com-

plete sample. These diameter and true strain rate values experimentally determined are therefore used to calculate the stress and then the elongational viscosity.

3.3. Steady and oscillatory shear experiments

A conventional strain-controlled rotational rheometer (Bohlin-VOR) was used in the cone-plate configuration to measure the steady and oscillatory viscosities. The full details of the rheometer are not shown in this work, but are given elsewhere (Macosko, 1984). To give an idea, the cylindrical polymer sample, typically 25 [mm] in diameter and 2 [mm] thick was sandwiched between steel discs, each 1.5 [mm] thick. The steel discs were heated by hot nitrogen gas streams, which were adjusted to give the desired melting and shearing temperatures before the start of a given series of experiments. The thermocouple that was used for oven control was positioned in the middle of the top plate. This minimized differences between the sample temperature and read-out values.

3.4. Elongational experiments

In addition to shear flows, extensional or stretching flow is important. In this experiment, an extensional rheometer (Instron) was used in the parallel plate mode to measure the load growth in uniaxial extensional flow. We should note that Troutons principle, Eqn. (1) (Tanner, 2000) extends to the circular sample cross section (Fig. 2). However, a new way of holding the sample and supporting it is used here compared to the conventional one. Thus, for a sample with initial length L_0 and L as the instantaneous length at uniform deformation, the Hencky strain can be expressed as:

$$\varepsilon = \ln\left(\frac{L}{L_0}\right) \tag{11}$$

Therefore the elongational strain rate is simply the rate of change of the strain with time:

$$\dot{\varepsilon} = \frac{d\varepsilon}{dt} = \frac{1}{L}\frac{dL}{dt} \tag{12}$$

If the sample is straining at the same rate everywhere along its length, then the local velocity of any element in cylindrical coordinates (Fig. 2) is given as:
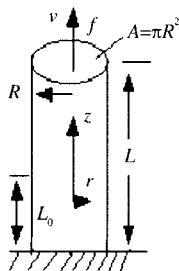

Fig. 2. A cylindrical sample being pulled at the top.

$$v_z = \dot{\varepsilon}z; \quad v_r = -\frac{1}{2}\dot{\varepsilon}r; \quad v_\theta = 0 \tag{13}$$

To achieve such a velocity field, the sample end must move with velocity

$$V = \dot{\varepsilon}L \tag{14}$$

Integrating (12) from L_0 to L, we obtain

$$L = L_0 e^{\dot{\varepsilon}t} \tag{15}$$

Substituting (15) into (14), the instantaneous velocity at the sample end becomes,

$$V = \dot{\varepsilon}L_0 e^{\dot{\varepsilon}t} \tag{16}$$

This shows that the length and the velocity of the end of sample increase exponentially when the strain-rate has a constant value throughout the test. The total strain or Hencky strain, ε, in the sample, is therefore dependent on time only and is given as

$$\varepsilon = \dot{\varepsilon}t \tag{17}$$

as in Eqn. (5).

As mentioned in the previous section, the only stress causing the sample to elongate is the one in the same direction as the moving sample or tensile stress. If we ignore surface tension and other factors like gravity for the moment, then this stress is the force or load, f, per unit area, A, acting on the end of the sample and is given by

$$\sigma_{zz} - \sigma_{rr} = \sigma_E = \frac{f}{A} \tag{18}$$

3.5. Diameter evolution

In traditional engineering practice, these quantities, σ_E and ε are defined relatively to the initial geometry of the specimen (nominal stress and strain). This means that the engineering definition is not representative of the local evolution of σ_E and ε, and cannot be used in any constitutive equation describing the actual behaviour of the material. As noticed, the sample local evolution is dependent on time; of course the specimen geometry and the force are also changing during the test, and consequently the local values of stress and strain.

Assuming that the deformation is globally homogeneous and the material is incompressible, the sample volume is therefore conserved so

$$D^2(t)L(t) = D_0^2 L_0 \tag{19}$$

In reality this deformation during the test can be localised only in the neck zone of the sample while other sections remain non-homogeneous. Thus, it becomes necessary to relate the true material behaviour during the test to the instantaneous local dimensions of the specimen (True diameter, True stress and True strain). We can define the
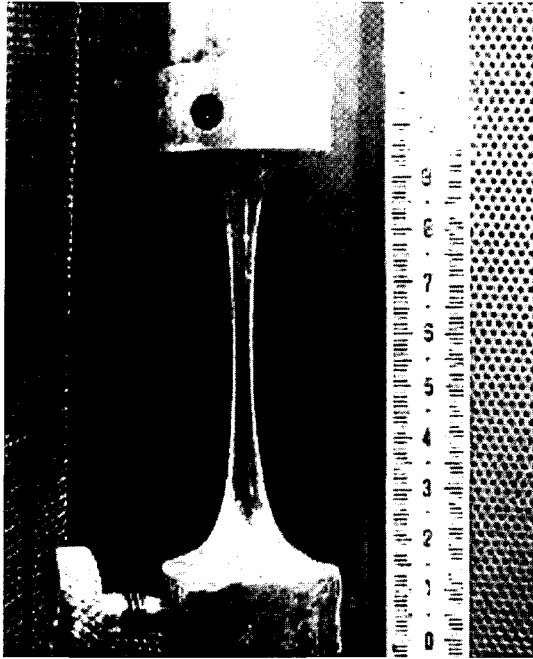
Fig. 3. Change in the diameter and length of polypropylene sample observed during elongational experiment using Instron instrument.
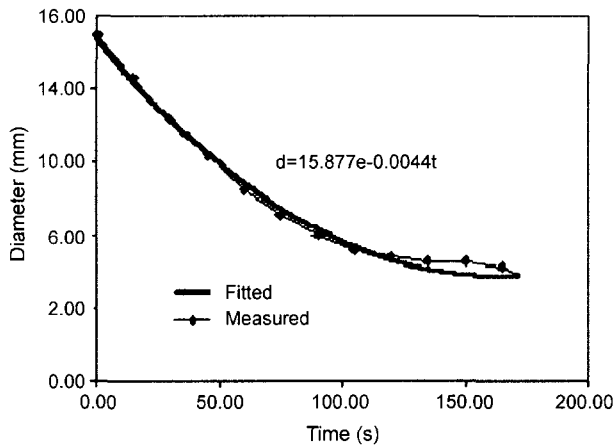

Fig. 4. Comparison between measured and fitted diameter evolution at different testing times.

true diameter in substituting (15) into (19). Hence,

$$D(t) = D_0 e^{-\frac{\dot{\varepsilon}}{2}t} \qquad (20)$$

This equation shows that the sample diameter exponentially decreases as the elongational time increases, Fig. 4. Practically, the determination of the curve (diameter-time) from (20) is not possible without knowledge of the true strain rate value. In reality this value does not remain constant throughout the test due to the change that happens in the sample diameter during elongation. To calculate the true diameter, Viana (1999) has used a method based on determining each strain rate value at different times. This

work develops an experimental technique for the direct determination of the average value of the strain-rate along the sample. This technique is based on analysing the complete testing image recorded from a digital camera. Particularly, the image of the test taken was completely downloaded to a computer as a movie. Thus, the true diameters at different testing time were measured by combining three different image-processing softwares and data obtained are used to build the curve diameter-time, illustrated in Fig. 4. Fitting of this curve gave an equation with the following form

$$D(t) = D_0 e^{-Ct} = 15.877 e^{-0.0044t} \qquad (21)$$

The extrapolation of the strain-rate value is obtain by comparing both (20) and (21). Hence,

$$\dot{\varepsilon} = 2C = 0.0088 \text{ s}^{-1} \qquad (22)$$

C is a constant value experimentally determined.

The measured strain rate $\dot{\varepsilon}$ is therefore a constant value. However, some errors are induced by the adopted experimental technique and the true strain value extrapolated showed a close approach to the experimental value imposed (0.009 s^{-1}) on the rheometer before the test.

Now it is easy to define the complete material stress response (true stress) as a dependence of σ_E on the time t elapsed since the stretching began:

$$\sigma_E(t) = \frac{4f}{\pi D^2(t)} \qquad (23)$$

Then, the true elongational viscosity, η_E, is determined by dividing the true stress by the true extensional rate. This is also a time dependent function and given by:

$$\eta_E(t) = \frac{\sigma_E(t)}{\dot{\varepsilon}} \qquad (24)$$

The magnitude of the gravitational effects can be considered. If the length of the thread is L, then gravitational stresses are at most of order $\rho g L$, which may be compared with the total axial stress, σ_E (Clearly gravitational stress varies along the thread, so at the central area, $\rho g L$ is certainly an overestimate of this stress).

From the results given in Fig. 5, we find gravitational stresses are at most of order of 10^3 Pa, whereas σ_E is of order 10^4 Pa. At lower extensions a similar ratio has been found. Therefore in what follows we shall ignore gravity.

3.6. True-stress evolution

The initial response of a polymer melt is elastic and might more appropriately be described in terms of the dependence of the stress on the time. For this reason, the stress generally increases more or less linearly as time progresses during the initial stages of the motion until a maximum point is reached, as shown the curve represented in Fig. 5. This point is associated with the beginning of
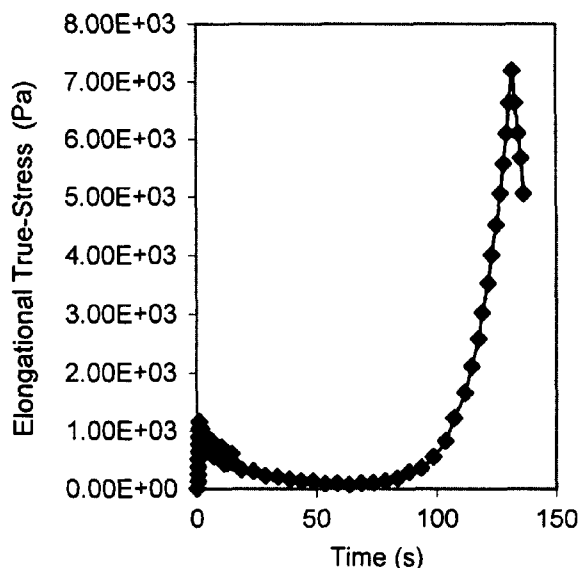
Fig. 5. The evolution of elongational True-stress versus time at 0.0097 s^{-1} elongational rate.

necking in the specimen and an apparent yielding. A load drop beyond "yield" indicates a decrease in true stress, accompanying neck formation and stabilization. The neck travels along the gauge section at a fairly constant flow or propagation true stress. Thus, from this point forward, strain hardening is manifested as an increase in true stress, usually when the neck proceeds into the wider sections towards the ends of the sample and then rupture occurs.

4. Results

Fig. 6 shows the evolution of sample deformation (sample diameter) at constant strain-rate and how this affects the flow (viscosity).
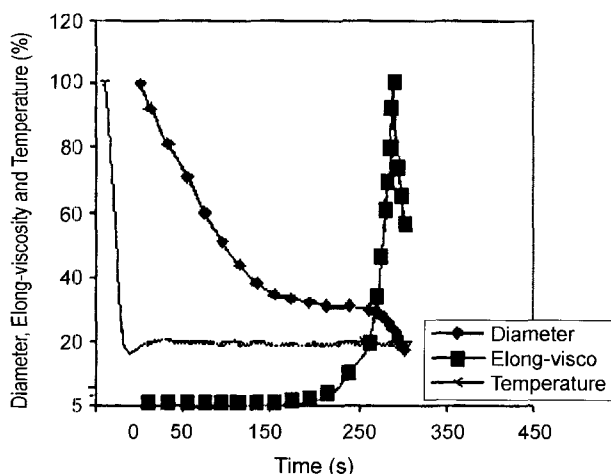
Fig. 6. Evolution of diameter (% of maximum diameter) and elongational viscosity (% of maximum viscosity) including temperature curve for 0.0047 s^{-1} strain-rate.
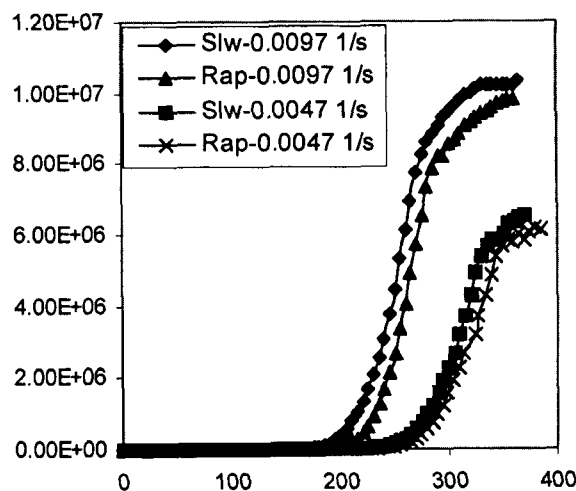
Fig. 7. Comparison between steady shear viscosities with sample cooled rapidly and slowly at 0.0097 s^{-1} shear rate.

Initially, a linear region is observed from the deformation curve. This region consists of both high elastic and viscous components of deformation. The viscous part plays an important role in the overall response of polymers in the linear deformation region. Consequently, the polymer response to the elongational deformation shows a low resistance to the deformation. On the other hand, with the occurrence of strain hardening, the elastic part of the polymer response to the elongation becomes predominant.

After the strain hardening reaches the maximum, a material break happens, which can be seen by the rapid decrease in the elongational viscosity and also in the sample diameter. While these changes in the diameter and viscosity are occurring, the temperature remains constant.

The cooling rate from the melting temperature to the shearing temperature should have an impact on crystallization. Fig. 7 compares the steady shear viscosity curves cooled at 48°C/min (rapid) and 8°C/min (slow) at the same shear rate, 0.0047 s^{-1} and also 0.0097 s^{-1}. Data reveal that the viscosity increase occurs slightly earlier when the sample is slowly cooled compare with the rapidly cooled one. Data also reveal that a big impact could be seen only with the increase of the deformation rate. While the shear rate is very small almost no impact is shown.

When the melted sample is cooled down (rapidly or slowly) to the crystallization temperature (130°C), some transient phenomena are always observed from temperature changes and it is important to stabilise prior to starting the test. The waiting time until equilibrium is reached is called the thermal equilibrium time. This is an important parameter, which should be also taken into consideration before a realistic crystallization experiment is to be done.

The presence of strain hardening is also influenced by this waiting time as shown in Fig. 8. Elongational data clearly reveal that the viscosity increase occurs eariler with
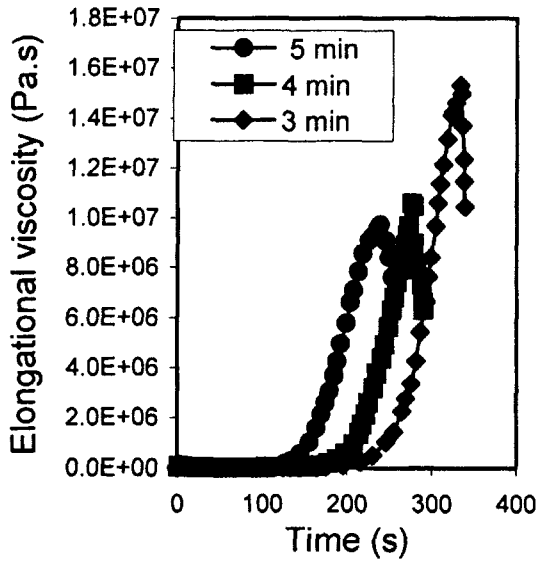
Fig. 8. The influence of thermal equilibrium time on steady elongational viscosity at 0.0041 s^{-1}.
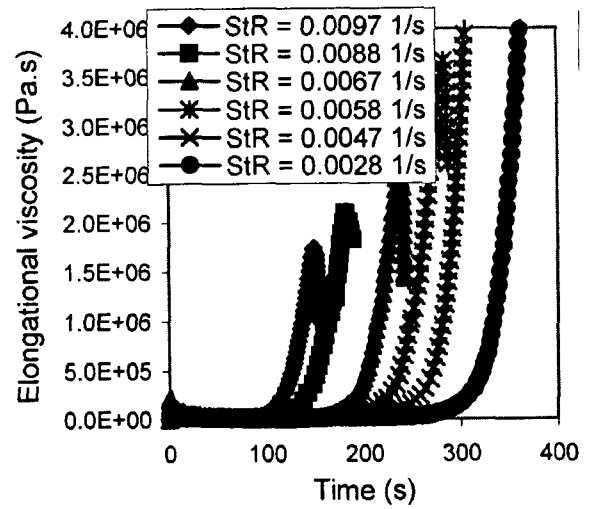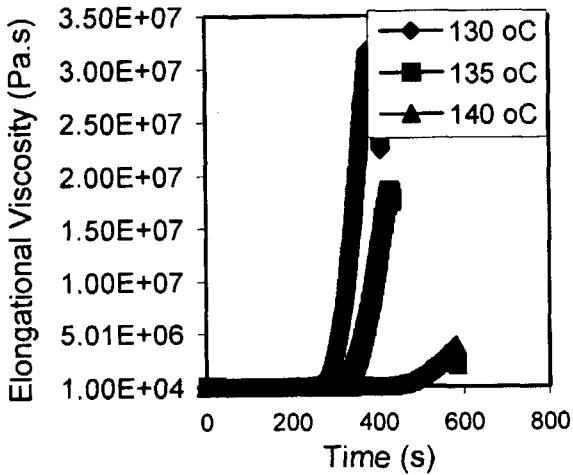

Fig. 9. Influence of temperature on crystallization for elongational strain-rate $= 0.0045 \text{ s}^{-1}$.

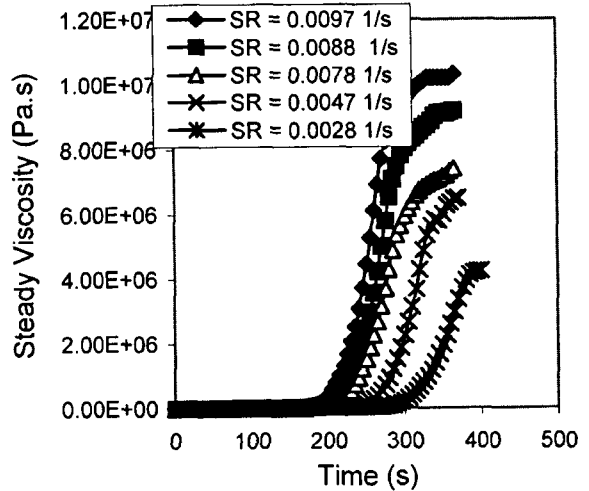**Fig. 10.** Elongational viscosity versus time at different deformation rates.

Fig. 11. Steady viscosity versus time at different shear rates.

a smaller maximum value as the waiting time is decreased.

We can observe in Fig. 9 that during the elongational flow, the crystallization temperature influences the increase of the viscosity at a given time. The decrease in the crystallization temperature shows an early increase and also a high value of viscosity, which allows a wide range of deformation rates to be experimented with.

These elongational viscosity data versus time at different elongational strain rates at 130°C are presented in Fig. 10. Initially, the elongational viscosity data for various elongational strain rates superimpose on the same curves for some time. Data reveal that at each strain rate there is a time (critical time) at which the start of rapid increase in the elongational viscosity (strain hardening) is observed. It can be seen that increasing the strain rate decreases the crit-

ical time and also the resistance to the deformation, which can be related so a low stretching means a low viscosity value.

Fig. 11 shows the influence of different shear-rates on viscosity growth for the steady simple shear measurement. The results reveal that during shearing, the time scale of shear-induced crystallization strongly depends on the shear rate. Data reveal the time at which the rapid viscosity growth decreases with increasing shear rate.

The comparison between the elongational and steady shear viscosities is shown in Fig. 12 and this comparison was realised choosing four different deformation rates from each experiment. At the lower rates, 0.0028 and 0.0047 s^{-1}, the elongational and steady curves lead to the similar results regarding the time scale of the beginning of the viscosity increases, but the maximum values of these viscosity increases, comparing both experiments, are completely dif-
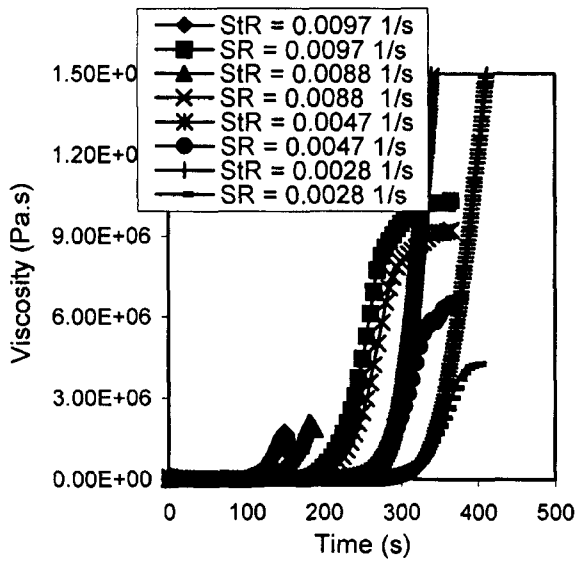
Fig. 12. Comparison between elongational and shear viscosities at different deformation rates (shear rate: SR and elongational rate: StR).
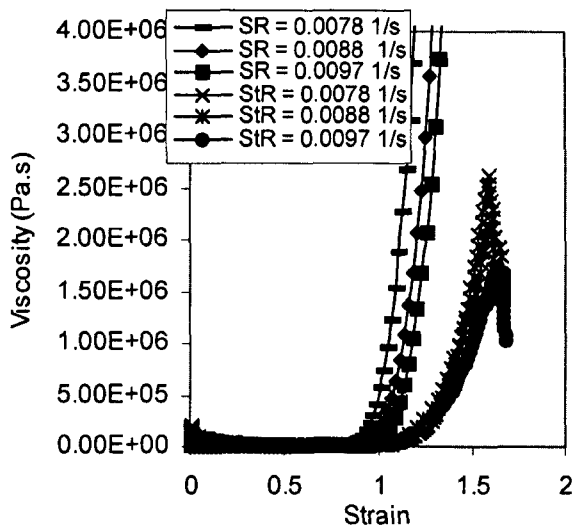

Fig. 13. Comparison between Hencky strain and shear strain at different deformation rates.

Fig. 14. Steady viscosity versus temperature at different shear rates.

Fig. 15. Comparison of crystallization behaviour with different strain values (Str) at 1 Hz in sinusoidal shearing.

ferent. The elongational values are about three times higher than the shear ones. Different histories were observed at high rates, 0.0088 and 0.0097 s⁻¹, the viscosity increase occurs earlier during elongational experiments and their maximum values are smaller compared to the steady shear experiments.

Fig. 13 shows elongational and shear viscosities at different elongational deformation rates plotted versus the Hencky strain. Hencky strains were calculated from Eqns (5) and (8). Data show that the onset of rapid shear and elongational viscosity growths occurred close to a critical value of the strain ranging between 1.1 − 1.2 approximately. These values are independent of strain-rate. Also
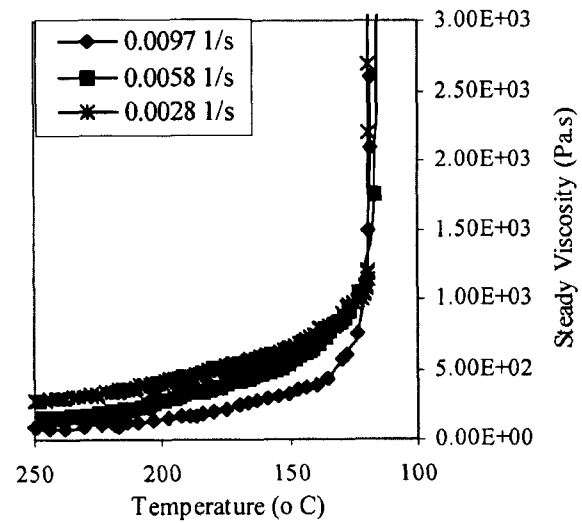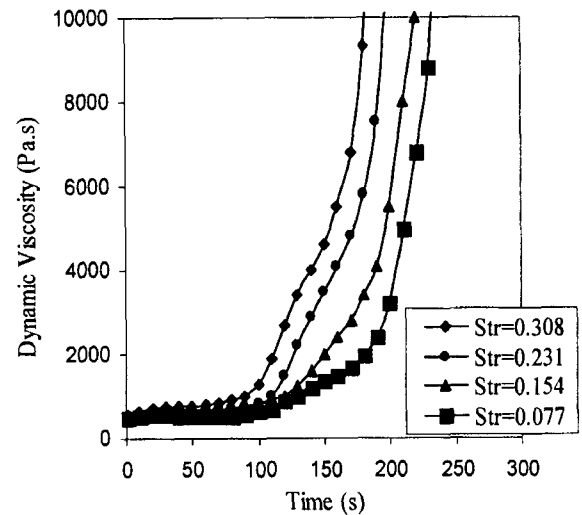
data show that the resistance to deformation, in the strain-hardening region, becomes more prominent with shearing than with elongation, which results in a high degree of stretching or high viscosity values occurring.

The steady viscosity versus temperature at different shear rates is presented in Fig. 14. In this experiment, we observed two different viscosity increases, the slow linear increase is due to the cooling rate and the faster (sudden) increase is due to the presence of strain hardening or crystallization and we found that the onset of crystallization occurs at about the same temperature. This could be seen by the fact that nearly all steady viscosity data for three different shear rates superimpose on the same curves at the beginning of steady viscosity growth.

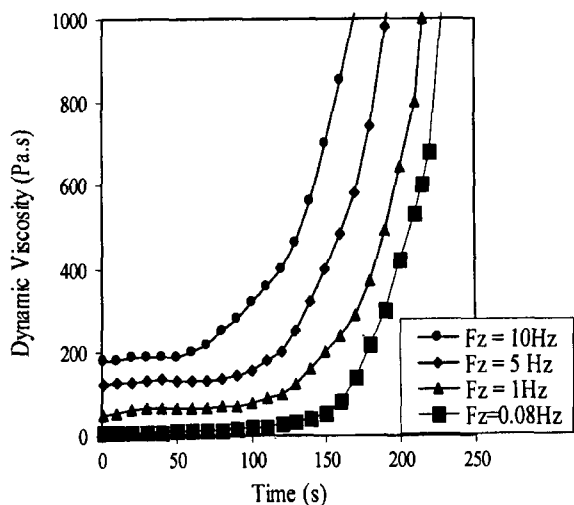Fig. 15 presents the dynamic viscosity (G''/ω) for oscillatory measurement at various oscillatory shear strains

Fig. 16. Influence of the frequency on the isothermal crystallization at a constant strain, 0.154.

plotted as a function of time. The results shown that at a given shear strain there is a critical time above which oscillatory viscosity begins to increase. As reported earlier this increase of viscosity is due to the onset of crystallisation.

The influence of the frequency on the crystallisation process was investigated, as shown in Fig. 16. The measurements were realised for different values such as: 0.08 Hz, 1 Hz, 5 Hz and 10 Hz, at a constant shear strain equal to 0.154. Data show that the start-up viscosity value and also the induction time to initiate viscosity growth depend on the shear frequency. For example, when the frequency is 10Hz, it is shown that the start-up viscosity value increases while the induction time decreases compared to the 0.08Hz one. This also shows that the onset of crystallisation happens earlier at the high value of frequency than at the lower frequency.

5. Discussions and conclusion

Over the range of conditions investigated in this study, it appears that even at relatively low shear or elongational rates viscosity growth (strain-hardening) phenomena can be observed. The onset of the strain hardening occurred, quite soon after transient start-up effects had subsided. Accordingly, it is possible that extension of chain segments during the start-up of flow (shear or elongation) may have governed the kinetics of this phenomenon.

Data clearly show that the onset of shear viscosity growth compared to the elongational one occurs at the same time value only for very small deformation rates. This seems to justify the theory established to describe the relation (1).

The comparison between shear and elongational Hencky strains shows the appearance of two very close critical strain values and it seems plausible that in addition to the

deformation rates, the strain could be another important parameter to be related to the structural changes in the macromolecular network.

The method used for the extrapolation of the average strain rate is qualitatively consistent although some imperfections were found. Consider first the cooling rate down to the crystallization temperature, although, as was shown in Fig. 7, the cooling rate has only a big impact with increase of the deformation rate. While the shear rate is very small no impact is shown, and use of faster cooling rate from a nitrogen environment is recommended for future tests. We believe that the main parameters, which could have considerable influence, are thermal equilibrium time and crystallization temperature. As shown in Figs. 8 and 9, changing these parameters has a great impact on the onset of the viscosity growth data. Consequently, they must be taken especially in account before further experiments are considered.

In conclusion, results of this study on shear and elongational-accelerated crystallization are consistent, at least in a qualitative sense. However, interpretation of the observed results on the basis of microstructure changes might appear to be inconsistent with the method used to detect the onset of crystallization, namely, a rise in the shear (steady and oscillatory) and elongational viscosities (Boutahar *et al.*, 1998). Thus, a deeper rheological study in combination with microscopy is recommended for a better understanding and also interpretation of different phenomena observed.

Acknowledgements

References

Bashir, Z., J. A. Odell and A. Keller, 1984, High modulus filaments of polyethylene with lamellar structure by melt processing; the role of the high molecular weight component, *J. Materials Science* **19**, 3713-3725.

Boutahar, K., C. Carrot and J. Guillet, 1998, Crystallization of polyolefins from rheological measurements. Relation between the transformed fraction and the dynamic moduli, *Macromolecules* **31**, 1921-1929.

Chai, C.K, Q. Auzoux, H. Randrianatoandro, P. Navard and J. M. Haudin, 2003, Influence of pre-shearing on the crystallization of conventional and metallocene polyethylenes, *Polymer* **44(3)**, 773-782.

Cunha, A. M., J. S. Godinho and J. C. Viana, 2000, Structure Development during polymer processing, edited by Cunha, A. M. and Stoyko Fakirov, 255-275, Kluwer Academic Publishers, Dordrecht, The Netherlands.

Han C. D., 1974, Rheology in polymer processing, *J Appl. Polym. Sci.* **18**, 3581.

Hoffman, J. D. and J. I. Jr. Lauritzen, 1961, Crystallisation of bulk polymers with chain folding: theory of growth of lamellar spherulites, *J. Res. Natl. Bur. Stand.* **65A**, 297-336.

Keller, A. and J. W. H. Kolnaar, 1997, Flow-induced orientation and structure formation, In H. E. H. Meijer, editor, Processing of polymers, volume **18** of Material Science and Technology: A Comprehensive treatment, chapter **4**, 189-268, VCH.

Koscher, E. and R. Fulchiron, 2002, Influence of shear on polypropylene crystallization: morphology development and kinetics, *Polymer* **43**, 6931-6942.

Kumaraswamy, G., A. M. Issaian and J. A. Kornfield, 1999, Shear-enhanced crystallization in isotactic polypropylene. 1. Correspondence between in situ rheo-optics and ex situ structure determination, *Macromolecules* **32**, 7537-7547.

Lagasse, R. and B. Maxwell, 1976, An experimental study of the kinetics of polymer crystallization during shear flow. *J. Polym. Eng. Sci.* B **16**, 189-199.

Lauritzen, J. I. Jr. and J. D. Hoffman, 1960, Theory of formation of polymer crystals with folded chains in dilute solution, *J. Res. Natl. Bur. Stand.* A **64**, 73-102.

Mackley, M.R. Frank, and A. Keller, 1975, Flow-induced crystallization of polyethylene melts. *J. Materials Science* **10**, 1501-1509.

Macosko, C. W., 1984, Rheology: principles, measurements and applications, Wiley-VCH, New York.

Petermann, J., M. Miles and H. Gleiter, 1979, The crystalline core of the row structures in isotactic polystyrene, (i). Nucleation and growth, *J. Polymer Science* **17**, 55-62

Tanner, R. I., 2000, Engineering Rheology, 2nd edition, Clarendon Press, Oxford.

Tanner, R. I., 2002a, A suspension model for low shear rate polymer solidification, *J. Non-Newtonian Fluid Mechanics* **102**, 397-408.

Tanner, R. I., 2002b, Note on the beginnings of sinusoidal testing methods, *Korea-Australia Rheol. J.* **14(2)**, 87-90.

Viana, J. M., 1999, Mechanical characterisation of injection moulded plates, Ph.D thesis, University of Minho.

Vleeshouwers, S. and H. E. H. Meijer, 1996, A rheological study of shear induced crystallization, *Rheol. Acta* **35**, 391-399.

Wassner, E. and R. D. Maier, 2000, Shear-induced crystallisation of polypropylene melts, XIIIth International Congress on Rheology, Cambridge, UK, **1**, 183-185.